

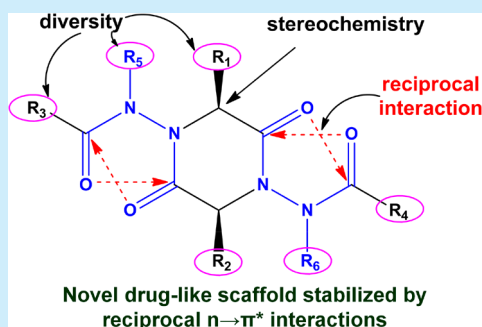
N,N'-Di(acylamino)-2,5-diketopiperazines: Strategic Incorporation of Reciprocal $n \rightarrow \pi^*$ Interactions in a Druglike Scaffold

Abdur Rahim,¹ Biswajit Sahariah,¹ and Bani Kanta Sarma^{*,1}

Department of Chemistry, School of Natural Sciences, Shiv Nadar University, Dadri, Uttar Pradesh 201314, India

S Supporting Information

ABSTRACT: The incorporation of the recently discovered reciprocal $n \rightarrow \pi^*$ interactions in 2,5-diketopiperazines (DKPs) is reported to design a novel *N,N'*-di(acylamino)-2,5-diketopiperazine (daa-DKP) scaffold. The design, synthesis, and structural features of daa-DKPs and the effect of reciprocal $n \rightarrow \pi^*$ interactions in their structural rigidity is discussed.



$n \rightarrow \pi^*$ interaction where the lone pair of electrons on a donor atom is delocalized into the antibonding π orbital of an acceptor group has attracted a lot of attention in recent years due to its ability to affect the geometries of both small and macromolecules.¹ For example, carbonyl–carbonyl ($\text{CO}\cdots\text{CO}$) $n \rightarrow \pi^*$ interaction is known to stabilize small molecules of biological significance such as aspirin and *N*-acylhomoserine lactones.² ($\text{CO}\cdots\text{CO}$) $n \rightarrow \pi^*$ interactions also influence the three-dimensional structures of polyesters, peptoids, and peptides.³ The emergence of $\text{CO}\cdots\text{CO}$ $n \rightarrow \pi^*$ interaction as a stabilizing force in α -helices, polyproline II (PPII) helices and collagen triple helices has created a lot of excitement in this area and the scientific community now considers $n \rightarrow \pi^*$ interaction as an important noncovalent interaction that warrants incorporation in the computational force fields.⁴ In recent years, amide–aromatic $n \rightarrow \pi^*_{\text{Ar}}$ interactions have also been effectively used to impart conformational rigidity in peptoids by controlling the *cis*–*trans* equilibrium of their tertiary amide bonds.^{3c,e,f,5} Despite their growing importance, to the best of our knowledge, there has been no attempt to systematically incorporate $n \rightarrow \pi^*$ interactions to design and stabilize any small molecule drug-like scaffold around which combinatorial libraries could be made and screened for identification of bioactive molecules. It is not clear if a scaffold derived by incorporating a small fragment that is known to participate in $n \rightarrow \pi^*$ interaction would produce library molecules having $n \rightarrow \pi^*$ interaction retained in them. And if so, would it be possible to tune the magnitude of the noncovalent interaction to impose rigidity and get control over the conformational stability of the molecules in the library? Herein, we take 2,5-diketopiperazine (DKP), a privileged scaffold, as our candidate of choice to investigate these possibilities.

We focused on 2,5-DKP as it offers numerous advantages as a drug scaffold.⁶ 2,5-DKPs are conformationally rigid, cell

permeable, and proteolytically stable small molecules found in many natural products and bioactive compounds. The small and semirigid 2,5-DKP core is ideal for designing highly diverse and stereochemistry controlled combinatorial libraries of druglike small molecules that obey the Lipinski rules.⁷ Recently, GlaxoSmithKline compound epelsiban (GSK-557,296-B), a 2,5-DKP-based orally bioavailable oxytocin receptor antagonist, was approved by the FDA for treatment of premature ejaculation in men.⁸ Many research groups have also explored various DKP analogues such as peptoid-DKPs,⁹ aza-DKPs,¹⁰ diketomorpholines (DKMs),¹¹ and aza-DKMs¹² as potential sources of bioactive molecules.

Recently, we reported the presence of reciprocal $\text{CO}\cdots\text{CO}$ $n \rightarrow \pi^*$ interactions in small molecules and proteins.¹³ For example, the two carbonyl groups of *N,N'*-diacylhydrazines (Figure 1A) orient in an arrangement favorable for reciprocal $\text{CO}\cdots\text{CO}$ interactions.¹³ We envisaged that incorporation of the *N,N'*-diacylhydrazine fragment into the 2,5-DKP scaffold (Figure 1B) could retain the reciprocal $\text{CO}\cdots\text{CO}$ interaction. This endeavor led to the design and synthesis of a novel *N,N'*-di(acylamino)-2,5-diketopiperazine (daa-DKP) scaffold with several different sites for diversification (Figure 1C). In this paper, we describe their design, synthesis, and structural features and evaluate the role of reciprocal $n \rightarrow \pi^*$ interactions on their structural rigidity.

To synthesize daa-DKPs (Scheme 1), first, acylhydrazides were reacted with 2-bromoester (1) to generate compounds 2a–d. Compounds 2a–d were then reacted with bromoacetyl bromide in the presence of 2,6-di-*tert*-butylpyridine to form compounds 3a–d, which were then treated with 2 equiv of acylhydrazides at 80 °C to produce daa-DKPs (5a–j) probably

Received: August 1, 2018

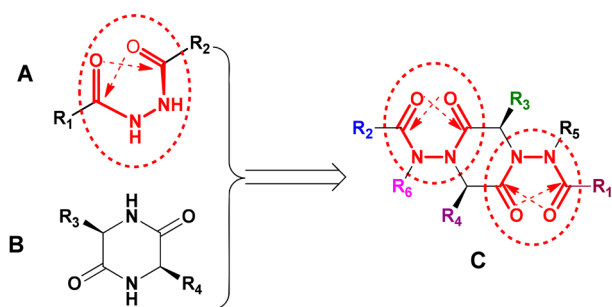
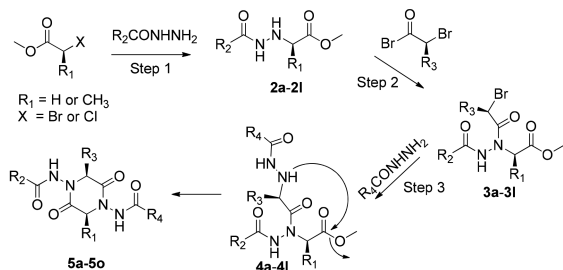


Figure 1. Incorporation reciprocal CO...CO interactions in DKPs. Chemical structures of (A) *N,N'*-diacylhydrazine, (B) 2,5-DKP, and (C) daa-DKP showing various possible positions of diversification. Broken arrows represent $n \rightarrow \pi^*$ interactions.

Scheme 1. Synthetic Route for daa-DKPs (**5a–n**)^a



5a: $R_1 = R_3 = H$, $R_2 = R_4 = Ph$; **5b:** $R_1 = R_3 = H$, $R_2 = R_4 = 4\text{-OMe-Ph}$
5c: $R_1 = R_3 = H$, $R_2 = R_4 = 4\text{-NO}_2\text{-Ph}$; **5d:** $R_1 = R_3 = H$, $R_2 = R_4 = 4\text{-CF}_3\text{-Ph}$
5e: $R_1 = R_3 = H$, $R_2 = Ph$, $R_4 = 4\text{-OMe-Ph}$; **5f:** $R_1 = R_3 = H$, $R_2 = Ph$, $R_4 = 4\text{-NO}_2\text{-Ph}$
5g: $R_1 = R_3 = H$, $R_2 = Ph$, $R_4 = 4\text{-CF}_3\text{-Ph}$; **5h:** $R_1 = R_3 = H$, $R_2 = 4\text{-OMe-Ph}$, $R_4 = 4\text{-NO}_2\text{-Ph}$
5i: $R_1 = R_3 = H$, $R_2 = 4\text{-OMe-Ph}$, $R_4 = 4\text{-CF}_3\text{-Ph}$; **5j:** $R_1 = R_3 = H$, $R_2 = 4\text{-NO}_2\text{-Ph}$, $R_4 = 4\text{-CF}_3\text{-Ph}$
5k: $R_1 = H$, $R_3 = CH_3$, $R_2 = Ph$, $R_4 = 4\text{-OMe-Ph}$; **5l:** $R_1 = H$, $R_2 = R_4 = Ph$, $R_3 = CH_3$
5m: $R_1 = H$, $R_2 = Ph$, $R_3 = CH_3$, $R_4 = 4\text{-Br-Ph}$; **5n:** $R_1 = R_3 = CH_3$, $R_2 = R_4 = Ph$
5o: $R_1 = R_3 = H$, $R_2 = R_4 = CH_3$; **5p:** $R_1 = R_3 = H$, $R_2 = R_4 = CF_3$

^aCompounds **5o,p** were used for computational analysis but not synthesized.

via compounds **4a–j** that we were not isolatable under the reaction conditions used. To incorporate chiral centers into the DKP ring (compounds **5k–m**; $R_3 = CH_3$), **2a** was reacted with *S*-2-methylbromopropionic acid in the presence of diisopropylcarbodiimide (DIC) at 37 °C to form **3e**, which was then treated with the corresponding acylhydrazides to produce **5k–m**. To synthesize **5n**, a daa-DKP having two chiral centers in the ring ($R_1 = R_3 = CH_3$), chiral 2-chloropropionic ester was used in the first step (see the [Supporting Information](#) for details). We observed that 2,6-di-*tert*-butylpyridine, a non-nucleophilic base, worked best in step 2 in which bromide displacement by base and intramolecular cyclization of **3** to form oxadiazinone could lead to side reactions. Further, to avoid oxadiazinone formation from **3**, we carried out step 3 in the absence of any external base. Note that the most common strategy¹⁴ of heating chloroacetamides in the presence of base to make 2,5-DKPs failed with chloro- and bromoacylated acylhydrazides due to their hydrolysis and intramolecular cyclization under these conditions.

We were able to grow single crystals of compounds **5a–f**, **5h**, **5m**, and **5n** and determine their solid-state structures. We found the daa-DKPs to pack either in tape (with two neighbors) or layer (with four neighbors) structures through intermolecular N–H...C=O hydrogen bonding (Figure 2A,B). The presence of an electron-donating group at the 4-position of the side-chain aromatic ring favored intermolecular hydrogen bonding through the side-chain carbonyl oxygen (**5b** and **5e**), whereas electron-withdrawing groups at the same

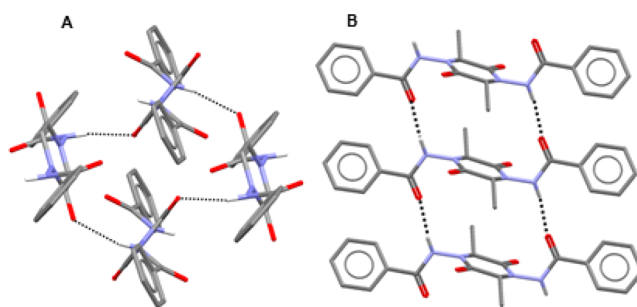


Figure 2. Crystal packing diagrams of daa-DKPs. (A) Layered packing in **5a** and (B) tape structure of **5n**.

position favored intermolecular hydrogen bonding through the ring carbonyl oxygens (**5c**, **5d**, **5f**, and **5h**) (Figure 3A,B and Figure S1). Therefore, by tuning the electronic environment around the side-chain amide groups, we could control the hydrogen bonding patterns in the daa-DKPs (Table S4).

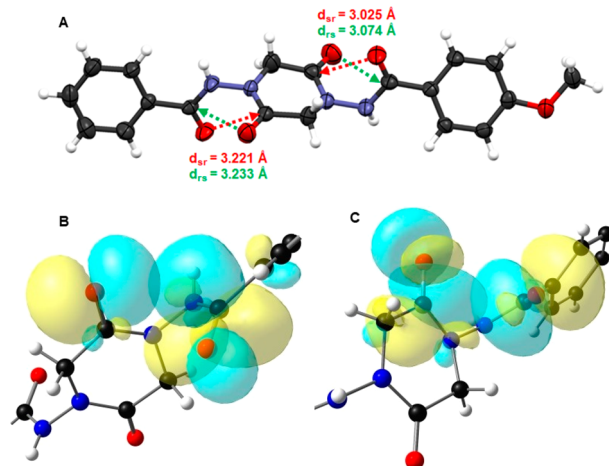


Figure 3. (A) Twisted arrangements of the carbonyl groups in **5e**. (B) NBO overlap diagram showing ring oxygen to side-chain $\pi^*_{C=O}$ donation and (C) side-chain oxygen to ring $\pi^*_{C=O}$ donation in **5e**. Only the 4-OMe-Ph side is shown.

We observed twisted arrangement between the ring and side-chain carbonyl groups of daa-DKPs ($C-N-N-C \sim \pm 80^\circ$), orientations expected for molecules having reciprocal CO...CO interactions.¹³ X-ray crystallographic O...C distances (d_{r-s} and d_{s-r}) shorter than 3.22 Å (the sum of van der Waals radii between C and O)¹⁵ and O...C=O angles (θ_{r-s} and θ_{s-r}) of $85 \pm 10^\circ$ indicate the presence of reciprocal CO...CO interactions in them (Table 1).¹³ Natural Bond Orbital (NBO)¹⁶ analysis of crystal geometries of the daa-DKPs also indicated the presence of reciprocal $n \rightarrow \pi^*$ interactions in them (Table 1). We observed stronger reciprocal $n \rightarrow \pi^*$ interactions when the side-chain aromatic ring contained an electron-donating or -withdrawing group at the 4-position. For example, in **5c**, the presence of an electron-withdrawing group (NO_2) increased the acceptor ability of the side-chain carbonyl π^* orbital and $n \rightarrow \pi^*$ interaction from the ring carbonyl oxygen lone pairs to the side-chain carbonyl π^* orbital ($E_{r-s} = 0.35 \text{ kcal}\cdot\text{mol}^{-1}$) (Table 1). Interestingly, an increase in donation from ring carbonyl to side-chain carbonyl increased the donation from side-chain carbonyl to ring carbonyl and vice versa. We also observed weak $\pi \rightarrow \pi^*$ interactions

Table 1. X-ray Crystallographic Parameters and NBO Energies Showing Reciprocal CO...CO Interactions^{a,b}

compd	d_{r-s} (Å)	θ_{r-s} (deg)	Θ_{r-s} (deg)	d_{s-r} (Å)	θ_{s-r} (deg)	Θ_{s-r} (deg)	$E_{r-s(n \rightarrow \pi^*)}$ (kcal·mol ⁻¹)	$E_{s-r(n \rightarrow \pi^*)}$ (kcal·mol ⁻¹)	E_T (kcal·mol ⁻¹)
5a	3.211	87.2	-1.46	3.209	87.2	0.41	0.14	0.14	0.40
5b	3.174	91.5	-0.13	3.209	90.3	1.23	0.26	0.08	0.54
5c	3.171	90.6	0.92	3.206	88.7	-0.64	0.35	0.12	0.61
5d	3.211	87.5	3.18	3.143	90.7	2.31	0.20	0.21	0.59
5e	3.074, 3.233	82.9, 87.4	1.79, -1.36	3.025, 3.221	85.3, 88.1	2.10, 1.28	0.26, 0.10	0.19, NP	0.60
5f	3.193, 3.266	86.8, 88.8	-1.21, -1.40	3.208, 3.257	85.8, 89.0	0.04, 0	0.08, NP	0.07, NP	0.15
5h	3.450, 3.249	96.1, 92.9	2.85, 1.73	3.418, 3.241	97.6, 93.2	1.26, 1.83	NP, 0.11	NP, NP	0.22
5m	3.336, 3.226	91.7, 89.6	-0.53, 0.98	3.322, 3.232	92.4, 89.4	1.94, 2.89	NP, 0.11	NP, NP	0.11
5n	3.122	88.0	1.27	3.073	90.5	1.37	0.38	0.46	1.14

^aThe calculations were done at the MP2/6-311+G(2d,p) level of theory. ^bKey: d_{r-s} , distance between ring carbonyl O to side-chain carbonyl C in angstroms (Å); d_{s-r} , distance between side-chain carbonyl O to ring carbonyl C in angstroms (Å); θ_{r-s} , angle from ring carbonyl O to side-chain C=O bond in degrees (deg); θ_{s-r} , angle from side-chain carbonyl O to ring C=O bond in degrees (deg); $E_{r-s(n \rightarrow \pi^*)} = n \rightarrow \pi^*$ second-order perturbation energy for donation from ring carbonyl O lone pair to side-chain carbonyl π^* orbital ($\pi^*_{C=O}$); $E_{s-r(n \rightarrow \pi^*)} = n \rightarrow \pi^*$ second-order perturbation energy for donation from side-chain carbonyl O lone pair to ring carbonyl π^* orbital ($\pi^*_{C=O}$); Θ_{r-s} , pyramidalicity of side-chain carbonyl C in degrees (deg); Θ_{s-r} , pyramidalicity of ring carbonyl C in degrees (deg); $E_T = [E_{r-s(n \rightarrow \pi^*)} + E_{s-r(n \rightarrow \pi^*)} + E_{r-s(\pi \rightarrow \pi^*)} + E_{s-r(\pi \rightarrow \pi^*)}]$. The stabilization energies of $\pi \rightarrow \pi^*$ interaction are taken from Table S6. NP = not present at 0.05 kcal·mol⁻¹ threshold.

between the carbonyl pairs of the daa-DKPs (Table S6). Among the daa-DKPs studied here, the strongest reciprocal interactions were observed in 5n having two chiral centers within the DKP ring. This observation opens the possibility of modulating $n \rightarrow \pi^*$ interactions by varying the substituents within the DKP ring. We did not find a strong correlation between pyramidalicity (Θ) of the acceptor carbonyl carbons and the nonbonded O...C distances. However, a positive pyramidalization of the acceptor carbon toward the donor oxygen was observed when the O...C distances were significantly shorter than 3.22 Å (Table 1, Figure S2).

It should be noted that incorporation of a motif having reciprocal $n \rightarrow \pi^*$ interaction may not always lead to molecules with the interactions intact as evidenced from the crystal geometries of 2a, 3a, 3c, and 3f, where no reciprocal interactions were observed (Figure S4–S7). For diacylhydrazines that show reciprocal interactions,¹³ the N–N–C=O torsion angles should be $\sim 0^\circ$. In daa-DKPs, the ring amide group is locked in the *cis*-conformation with respect to the N–N bond (N–N–C=O $\sim 0^\circ$), whereas the side-chain amide group is locked in the *trans*-conformation with respect to the NH group (H–N–C=O $\sim 180^\circ$) due to steric reasons, which orients the carbonyl groups for a favorable reciprocal interaction.

We hypothesized that the magnitude of reciprocal interactions could play a role in determining the conformational preference of the DKP ring. However, we observed that the symmetric daa-DKPs crystallized in centrosymmetric space groups with chair or planar DKP ring conformation while the asymmetric ones crystallized in the boat form independent of the strength of reciprocal interactions (Table S4). As the reciprocal interactions are weak, packing forces could possibly overcome them to crystallize the molecules in the more symmetrical forms. Theoretical calculations in the gas phase for isolated daa-DKP molecules show that the reciprocal interactions are stronger in boat form. The gas phase calculations also suggest that the boat forms (C_2) of the DKP rings are more stable than the chair or planar forms (C_i) for all the daa-DKP molecules (Table 2, Table S5). Nevertheless, based on symmetry and energetics, we can make a priori prediction that the centrosymmetric daa-DKPs would crystallize in the chair or planar conformation of the DKP ring whereas noncentrosymmetric ones would crystallize

Table 2. Zero-Point Energy Corrected Electronic Energy $\Delta(E + ZPE)$ of daa-DKPs Calculated Using B3LYP, M06-2X, and MP2 Methods and 6-31G(d) and 6-311+G(2d,p) Basis Sets^a

compd	PG	$\Delta(E + ZPE)$ (kcal·mol ⁻¹)		
		B3LYP	M06-2X	MP2
5a	C_i	0.0 ^b (0.0 ^b)	0.34 (0.82)	ND (0.95)
	C_2	0.68 (0.45)	0.0 (0.0)	ND (0.0)
5b	C_i	0.0 ^b (0.0 ^b)	0.39 (0.59 ^b)	ND (0.97)
	C_2	1.84 (1.92)	0.0 (0.0)	ND (0.0)
5c	C_i	0.0 ^b (0.0 ^b)	0.67 (0.75)	ND (0.99)
	C_2	0.58 (0.25)	0.0 (0.0)	ND (0.0)
5o	C_i	0.0 ^b (0.0)	0.52 (0.82)	0.66 (1.07)
	C_2	0.39 (0.01)	0.0 (0.0)	0.0 (0.0)
5p	C_i	0.0 ^b (0.0)	0.85 (0.90)	0.89 (1.20)
	C_2	0.32 (0.29)	0.0 (0.0)	0.0 (0.0)

^aKey: PG, point group; ND, not determined, as the calculations could not be completed. Values in parentheses are obtained using 6-31G(d) basis set. ^bOptimized with C1 point group as the C_i point group resulted in an imaginary frequency.

in the more stable boat form. Accordingly, we observed chair conformation of DKP ring in 5a–d and 5n and boat conformation in 5e, 5h, and 5m (Table S4). Only in 5f, the DKP ring conformation was found to be different from our prediction.

Finally, reciprocal interactions, the repulsion between the nitrogen lone pairs, repulsion between the ring and side-chain carbonyl lone pairs, and other delocalization effects¹⁷ [$n_N \rightarrow \sigma^*_{C-N}$ and $n_N \rightarrow \sigma^*_{N-H}$ interactions; Table S14] should restrict free rotation around the N–N bonds in daa-DKPs. The high barrier (>20 kcal·mol⁻¹) of rotation around the N–N bond in 5a and 5p supports this assumption (Figure S3). As can be seen from Figure S3, the substituent on the side-chain amide group does not have significant effect on the barrier to N–N bond rotation, which will need further investigation. Due to the high N–N bond rotation, the side-chain and the ring carbonyl groups of daa-DKPs are found to be locked in an orientation favorable for reciprocal interactions (C–N–N–C $\sim \pm 80^\circ$). Further, the side-chain amide bond (H–N–C=O) geometry is expected to be locked in the *trans*-conformation due to steric reasons, which is also supported by their crystal

geometries. In addition, as observed for the asymmetric daa-DKPs, higher reciprocal interactions in the boat form should bias the DKP rings toward boat conformations. All these effects should make the daa-DKPs more rigid than the peptide-based DKPs.

In conclusion, we have shown that reciprocal $n \rightarrow \pi^*$ interactions could be strategically incorporated in a drug-like scaffold by conveniently synthesizing the daa-DKPs having reciprocal $n \rightarrow \pi^*$ interactions. To the best of our knowledge, this is the first study where strategic incorporation of $n \rightarrow \pi^*$ interaction has been carried out to design a druglike scaffold. The daa-DKP scaffold is ideal for combinatorial synthesis as it can be diversified and its stereochemistry can be controlled at multiple positions. Our experimental and theoretical data suggest that the daa-DKP molecules are rigid, a property which may be useful for binding to biological targets. Further, the hydrogen bond donor and acceptor units in the side-chain amide groups in daa-DKPs should provide additional sites for engagement with biological targets such as proteins and DNA. Finally, as these are low molecular weight compounds that follow Lipinski rules, they are potential candidates to be included in orally bioavailable drug discovery campaigns.

■ ASSOCIATED CONTENT

Supporting Information

The Supporting Information is available free of charge on the ACS Publications website at DOI: [10.1021/acs.orglett.8b02449](https://doi.org/10.1021/acs.orglett.8b02449).

Experimental procedures, ^1H and ^{13}C NMR spectra, X-ray crystallographic data, and computational data (PDF)

Accession Codes

CCDC 1844723–1844734 and 1844767 contains the supplementary crystallographic data for this paper. These data can be obtained free of charge via www.ccdc.cam.ac.uk/data_request/cif, or by emailing data_request@ccdc.cam.ac.uk, or by contacting The Cambridge Crystallographic Data Centre, 12 Union Road, Cambridge CB2 1EZ, UK; fax: + 44 1223 336033.

■ AUTHOR INFORMATION

Corresponding Author

*E-mail: banikanta.sarma@snu.edu.in.

ORCID

Abdur Rahim: 0000-0003-4236-6089

Biswajit Sahariah: 0000-0001-6649-892X

Bani Kanta Sarma: 0000-0003-0830-6007

Notes

The authors declare no competing financial interest.

■ ACKNOWLEDGMENTS

This project was funded by Shiv Nadar University (SNU) and an Early Career Research Grant (ECR/2015/000337) from the Science and Engineering Research Board (SERB), Department of Science and Technology (DST), Government of India. We acknowledge the MAGUS supercomputing facility at SNU.

■ REFERENCES

- (1) (a) Newberry, R. W.; Raines, R. T. *Acc. Chem. Res.* **2017**, *50*, 1838–1846. (b) Singh, S. K.; Das, A. *Phys. Chem. Chem. Phys.* **2015**, *17*, 9596–9612. (c) Paulini, R.; Müller, K. M.; Diederich, F. *Angew. Chem., Int. Ed.* **2005**, *44*, 1788–1805.
- (2) (a) Choudhary, A.; Kamer, K. J.; Raines, R. T. *J. Org. Chem.* **2011**, *76*, 7933–7937. (b) Newberry, R. W.; Raines, R. T. *ACS Chem. Biol.* **2014**, *9*, 880–883.
- (3) (a) Wang, S.; Shi, G.; Guan, X.; Zhang, J.; Wan, X. *Macromolecules* **2018**, *51*, 1251–1259. (b) Huang, Y.; Ferrie, J. J.; Chen, X.; Zhang, Y.; Szantai-Kis, D. M.; Chenoweth, D. M.; Petersson, E. J. *Chem. Commun.* **2016**, *52*, 7798–7801. (c) Newberry, R. W.; VanVeller, B.; Guzei, I. A.; Raines, R. T. *J. Am. Chem. Soc.* **2013**, *135*, 7843–7846. (d) Newberry, R. W.; Raines, R. T. *Chem. Commun.* **2013**, *49*, 7699–7701. (e) Laursen, J. S.; Engel-Andreasen, J.; Fristrup, P.; Harris, P.; Olsen, C. A. *J. Am. Chem. Soc.* **2013**, *135*, 2835–2844. (f) Stringer, J. R.; Crapster, J. A.; Guzei, I. A.; Blackwell, H. E. *J. Am. Chem. Soc.* **2011**, *133*, 15559–15567. (g) Choudhary, A.; Raines, R. T. *Protein Sci.* **2011**, *20*, 1077–1081. (h) Gorske, B. C.; Stringer, J. R.; Bastian, B. L.; Fowler, S. A.; Blackwell, H. E. *J. Am. Chem. Soc.* **2009**, *131*, 16555–16567. (i) Gorske, B. C.; Bastian, B. L.; Geske, G. D.; Blackwell, H. E. *J. Am. Chem. Soc.* **2007**, *129*, 8928–8929.
- (4) (a) Newberry, R. W.; Bartlett, G. J.; VanVeller, B.; Woolfson, D. N.; Raines, R. T. *Protein Sci.* **2014**, *23*, 284–288. (b) Bartlett, G. J.; Newberry, R. W.; VanVeller, B.; Raines, R. T.; Woolfson, D. N. *J. Am. Chem. Soc.* **2013**, *135*, 18682–18688. (c) Bartlett, G. J.; Choudhary, A.; Raines, R. T.; Woolfson, D. N. *Nat. Chem. Biol.* **2010**, *6*, 615–620. (d) Fufezan, C. *Proteins: Struct., Funct., Genet.* **2010**, *78*, 2831–2838.
- (5) Caumes, C.; Roy, O.; Faure, S.; Taillefumier, C. *J. Am. Chem. Soc.* **2012**, *134*, 9553–9556.
- (6) Borthwick, A. D. *Chem. Rev.* **2012**, *112*, 3641–3716.
- (7) (a) Lipinski, C. A. *Drug Discovery Today: Technol.* **2004**, *1*, 337–341. (b) Lipinski, C. A.; Lombardo, F.; Dominy, B. W.; Feeney, P. J. *Adv. Drug Delivery Rev.* **2001**, *46*, 3–26.
- (8) Borthwick, A. D.; Liddle, J.; Davies, D. E.; Exall, A. M.; Hamlett, C.; Hickey, D. M.; Mason, A. M.; Smith, I. E. D.; Nerozzi, F.; Peace, S.; Pollard, D.; Sollis, S. L.; Allen, M. J.; Woollard, P. M.; Pullen, M. A.; Westfall, T. D.; Stanislaus, D. J. *J. Med. Chem.* **2012**, *55*, 783–796.
- (9) (a) Suwal, S.; Kodadek, T. *Org. Biomol. Chem.* **2014**, *12*, 5831–5834. (b) Zuckerman, R. N.; Goff, D. N.; Simon, N. G.; Spear, K.; Scott, B.; Sigmund, A. G.; Goldsmith, R. A.; Marlowe, C. K.; Pei, Y.; Richter, L.; Simon, R. *PCT Int. Appl. WO1996040202A1*.
- (10) (a) Regenass, P.; Bosc, D.; Riché, S.; Gizzi, P.; Hibert, M.; Karmazin, L.; Ganesan, A.; Bonnet, D. *J. Org. Chem.* **2017**, *82*, 3239–3244. (b) Ivanovich, R. A.; Vincent-Rocan, J.-F.; Elkaed, E. B.; Beauchemin, A. M. *Org. Lett.* **2015**, *17*, 4898–4901. (c) Regenass, P.; Margathe, J.-F.; Mann, A.; Suffert, J.; Hibert, M.; Girard, N.; Bonnet, D. *Chem. Commun.* **2014**, *50*, 9657–9660. (d) Bonnet, D.; Margathe, J.-F.; Radford, S.; Pflimlin, E.; Riché, S.; Doman, P.; Hibert, M.; Ganesan, A. *ACS Comb. Sci.* **2012**, *14*, 323–334.
- (11) (a) Bassetto, M.; Ferla, S.; Pertusati, F.; Kandil, S.; Westwell, A. D.; Brancale, A.; McGuigan, C. *Eur. J. Med. Chem.* **2016**, *118*, 230–243. (b) Cingolani, G. M.; Di Stefano, A.; Mosciatti, B.; Napolitani, F.; Giorgioni, G.; Ricciutelli, M.; Claudii, F. *Bioorg. Med. Chem. Lett.* **2000**, *10*, 1385–1388. (c) Szardenings, A. K.; Burkoth, T. S.; Lu, H. H.; Tien, D. W.; Campbell, D. A. *Tetrahedron* **1997**, *53*, 6573–6593. (d) Cook, A. H.; Cox, S. F. *J. Chem. Soc.* **1949**, 2347–2351.
- (12) Berthet, M.; Legrand, B.; Martinez, J.; Parrot, I. *Org. Lett.* **2017**, *19*, 492–495.
- (13) Rahim, A.; Saha, P.; Jha, K. K.; Sukumar, N.; Sarma, B. K. *Nat. Commun.* **2017**, *8*, 78.
- (14) Cho, S.-D.; Song, S.-Y.; Kim, K.-H.; Zhao, B.-X.; Ahn, C.; Joo, W.-H.; Yoon, Y.-J.; Falck, J. R.; Shin, D.-S. *Bull. Korean Chem. Soc.* **2004**, *25*, 415–416.
- (15) Bondi, A. *J. Phys. Chem.* **1964**, *68*, 441–451.
- (16) Glendening, E. D.; Reed, A. E.; Carpenter, J. E.; Weinhold, F. *NBO Version 3.1*; University of Wisconsin: Madison.
- (17) (a) Yang, T.; An, J.-J.; Wang, X.; Wu, D.-Y.; Chen, W.; Fossey, J. S. *Phys. Chem. Chem. Phys.* **2012**, *14*, 10747–10753. (b) Singh, S. K.; Kumar, S.; Das, A. *Phys. Chem. Chem. Phys.* **2014**, *16*, 8819–8827.